Pergamon

Int. J. Solids Structures Vol. 33, No. 23, pp. 3477–3489, 1996

0020–7683/96 $15.00 + .00

0020–7683(95)00190–5

DISTRIBUTION OF CONTACT STRESSES ALONG A WORN FRETTING SURFACE

S. FAANES†
Department of Applied Mechanics, The Norwegian Institute of Technology, 7034 Trondheim, Norway

(*Received* 13 *September* 1994; *in revised form* 25 *July* 1995)

Abstract—Previous investigations have established fracture mechanics as a useful tool in quantitative studies of fretting fatigue crack behaviour. One major problem in such analyses is the difficulty in determining the distribution of stresses in the fretting contact. In this paper the contact pressure is expected to be uniform due to the wear of contact surfaces taking place in fretting. Based on this assumption analytical expressions for the stick zone, the slip amplitude and the distribution of shear stresses are found. It is seen that the distribution of contact shear stresses varies considerably with the size and location of the stick zone. This in turn affects the loading of the fretting cracks in terms of stress intensity factors, hence the behaviour of these cracks will vary with the degree of partial slip. When full slip takes place, the distributions of contact pressure and shear stress are uniform according to the model presented here. Copyright © 1996 Elsevier Science Ltd

1. INTRODUCTION

In order to improve the predictability of fretting fatigue failure in industrial components, a quantitative understanding of the fretting fatigue process is needed. One of the major problems of investigating these mechanisms is the large number of variables involved and how these can be monitored. The distribution of contact stresses is one of these variables.

Few investigations of fretting fatigue have treated the contact stress distribution and its influence on the fatigue behaviour. Edwards (1981) calculated fretting fatigue lives using different distributions and found that the distribution significantly affected the results. Tanaka *et al.* (1985) used a weighted combination of a uniform distribution and a concentrated force at the leading edge of the contact without stating any physical basis for this assumption. Switek (1984) assumed the contact pressure distribution to have a parabolic shape. Finite element analysis has been carried out by Hattori *et al.* (1988) and distributions of contact shear and pressure have been found for bridge pads and large stress concentrations were revealed at the pad edges. Probably the most careful treatment of the distribution of contact stresses in fretting fatigue has been carried out by O'Connor (1981) in the analysis of fretting occurring in a cylindrical contact, and later by Nowell and Hills (1987) who found that the tension of the specimen modifies the classical Mindlin solution to this contact problem. No corresponding analysis has been carried out for flat-ended fretting contacts where difficulties with infinite stresses and displacements arise in the elastic solutions.

The distribution of contact stresses across a contact zone is of course dependent on geometry and material properties of the components in contact. For industrial components geometry and materials are usually given, and a study of the fretting fatigue strength must be based on the knowledge of the stress distribution in each individual case. In experiments which aim to study mechanisms of fretting fatigue in general, the geometry and materials can be chosen to fit this purpose. Contact between two bodies is conveniently classified as either "complete" or "incomplete" which means that the size of the contact zone is either independent or dependent on the contact loading. Hills and Nowell (1992) proposed a fretting fatigue experiment using a Herzian contact, which is incomplete, where the contact stress distributions and slip zones can be obtained. Since the contact stress distribution is

† Presently at Kværner Energy a.s., PO Box 9277, Grønland, 0134 Oslo, Norway.

known, an important obstacle in investigating the mechanisms of fretting fatigue is eliminated. But many fretting fatigue experiments today use complete contacts. The numerous results available from these fretting experiments could be better exploited if the stress distribution were known.

The present paper discusses how flat-ended fretting surfaces may be modified by wear, and closed-form solutions, that describe the stress distribution as well as the amount of slip in the partial slip regime of such complete contacts, are developed. These results are used to discuss the relation between the loading in terms of the stress intensity factor of a fretting crack and the slip amplitude in the partial slip regime.

2. BACKGROUND

2.1. *Equations of plane contacts*

The equations and definitions presented below are found in *Mechanics of Elastic Contacts* by Hills *et al.* (1993) and readers wishing to study the background should refer to this text.

If contact is assumed between two semi-infinite bodies, the general equations for the relation between relative displacements and stress distributions in a contact zone are given as

$$\frac{1}{\pi}\int_{-a}^{a}\frac{p(s)\,\mathrm{d}s}{x-s}-\beta q(x)=\frac{1}{A}\frac{\mathrm{d}h}{\mathrm{d}x} \tag{1a}$$

$$\frac{1}{\pi}\int_{-a}^{a}\frac{q(s)\,\mathrm{d}s}{x-s}+\beta p(x)=\frac{1}{A}\frac{\mathrm{d}g}{\mathrm{d}x} \tag{1b}$$

where p is the distribution of contact pressure, q is the distribution of shear stress, x is the location along the surface. The width of the contact zone is $2a$, and h and g are the relative displacements between the two bodies in contact perpendicular and parallel to the contact surface, respectively. A and β are constants dependent on the material properties of the two materials as follows

$$A=\frac{\kappa_1+1}{4\mu_1}+\frac{\kappa_2+1}{4\mu_2} \tag{2a}$$

$$\beta=\frac{\mu_2(\kappa_1-1)-\mu_1(\kappa_2-1)}{\mu_2(\kappa_1+1)+\mu_1(\kappa_2+1)} \tag{2b}$$

where β is known as Dundurs' constant. The index 2 refers to the material properties of the body where the coordinate system is fixed (see Fig. 2), μ is the modulus of rigidity and $\kappa=(3-\nu)/(1+\nu)$ for plane stress and $\kappa=3-4\nu$ for plane strain. It is seen that if the material of the bodies 1 and 2 are interchanged the sign of β changes. Strictly, the integrals in eqns (1) can only be evaluated as Cauchy Principal Values when a singularity occurs in the integration range. It is seen that if $\beta=0$ eqns (1) are uncoupled which simplifies the solution of the problem considerably. The materials are defined to be *similar* when this is the case (e.g. when the same material is used in both bodies in contact, or when two incompressible bodies under plane strain conditions are used). For steel pressed against duraluminium $\beta=-0.11$ [Table 2.2, Hills *et al.* (1993)].

It should be noted that in most fretting fatigue experiments, body 2 (i.e. the specimen) is exposed to a load parallel to the contact surface. When this causes an additional strain, ε_2, to occur in the specimen, eqn (1b) must be modified thus

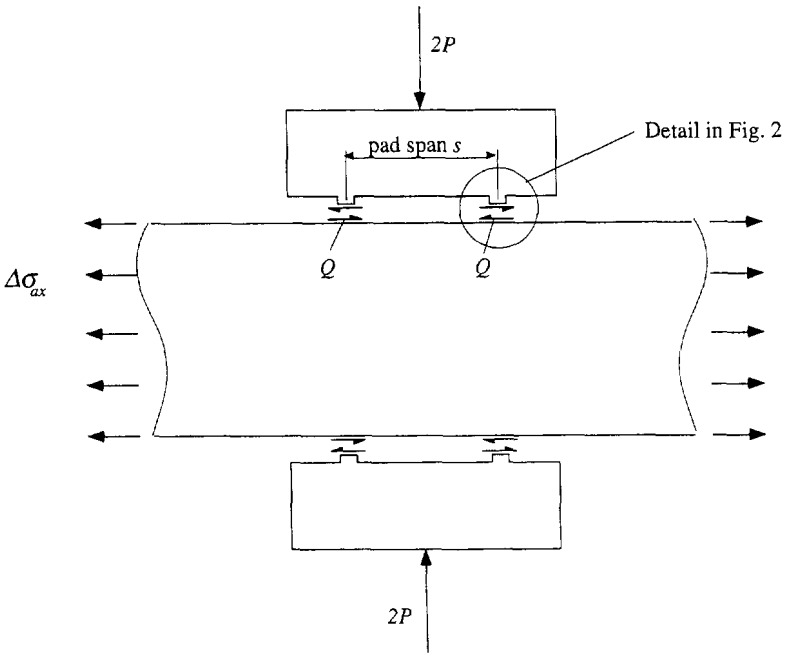

Fig. 1. Principal configuration of a fretting experiment with "bridge pads."

$$\frac{1}{\pi}\int_{-a}^{a}\frac{q(s)\,\mathrm{d}s}{x-s}+\beta p(x)=\frac{1}{A}\left(\frac{\mathrm{d}g}{\mathrm{d}x}-\varepsilon_2\right).$$

As discussed by Nowell and Hills (1987), this causes a shift in the stick zone eccentricity for the load levels discussed in this paper, as well as a slightly modified stress distribution in the stick zone. Mathematical techniques to find $p(x)$ and $q(x)$ in eqns (1) are also presented by Hills *et al.* (1993), and the class of solutions which will be needed is quoted in the appendix in the present paper.

2.2. *The "bridge-type" fretting contact*

Many fretting experiments, such as those described by Edwards (1981), Nix and Lindley (1988) and Fernando *et al.* (1994), use two bridge pads with flat (i.e. complete) contact surfaces clamped to the specimen as illustrated in Fig. 1. Fretting damage is produced by exposing the specimen to a push–pull cyclic load. Due to the deformation of the specimen, a relative movement is enforced between the pad and the specimen. As a result of the high stress concentrations at the edges of the fretting pad, the surface of either the specimen or the fretting pad—or both—are worn so that the stress concentration is reduced. In all experiments referred to above, it is seen that during a certain number of fretting cycles in the beginning of an experiment, the friction force gradually increases until it stabilizes at a certain plateau. The increase in frictional forces is explained by the development of local yielding and welding in the contact which after a while produce wear debris that functions as a lubricator. When the frictional force plateau is reached, a stationary situation is obtained with a modified contact geometry and a balance of debris worn off the surfaces and transported away from the contact zone.

In the following, it is assumed that the contact pad can be modelled as either completely rigid or as a half-plane body, while the specimen is treated as the latter. If the pad is stiffer than the specimen, the pad can be modelled as a rigid flat-ended punch while the modulus of rigidity and the Poisson's ratio are adjusted to keep A and β constant. Since the distribution of contact shear stresses is proportional to the contact pressure distribution in such a flat-ended rigid punch, Hills and Nowell (1994) argued that no slip takes place takes place until the whole contact slides and the shear force Q equals the friction limit, fP, where f is the coefficient of friction and P is the contact normal force. To model the pad as a rigid

punch is impossible when the same material is used in the pad and the specimen, but if the assumption of half-plane bodies holds for the pad as well as the specimen, the same solution to the distribution of stresses is obtained, and the argument of Hills and Nowell (1994) is still valid. Experiments carried out by Edwards (1981) also showed that full slip took place in the first cycles of a fretting test. This implies that the increase of the friction force can only be caused by an increase in the friction coefficient, f, since the contact pressure P is kept constant. As the pad slides back and forth in the oscillating fretting process, the surface (of the specimen, of the pad or both) is expected to wear to a shape that gives a uniform pressure and shear stress according to Dundurs and Comninou (1980). This shape is found from eqn (1a) by setting $p(x) = p_0$:

$$h(x) = -\frac{Ap_0}{\pi}\left[(a+x)\ln\left(1+\frac{x}{a}\right)+(a-x)\ln\left(1-\frac{x}{a}\right)+\beta f x\right] \tag{3}$$

giving the difference $h_{\max}-h_{\min} = h(0)-h(a) = a(2\ln 2Ap_0/\pi+\beta f)$ as a measure of the depth of a wear scar in a fretting zone. This shape is obtained when the friction force reaches its plateau.

It is shown in Section 3 in this paper that if the friction force is sufficiently small, partial slip will occur in the new wear modified contact geometry described by eqn (3). For the experimental procedure used by the investigators referred to above, reducing the axial loading would cause a decrease of the full slip amplitude. A reduction of the friction force could be obtained by reducing the axial loading below the point where the measured full slip disappears. Therefore, controlled partial slip conditions can be obtained in such experiments if the friction force Q is measured so that the ratio Q/fP is known.

Edwards (1981) discovered that after approximately 1% of the fatigue life the macro slip either disappeared entirely or continued unchanged during the fatigue life. This indicates that depending on the axial load, contact pressure and pad span used in the fretting test, the ratio Q/fP will either remain unity (full slip), or drop such that a stick zone will appear somewhere under the pad even without a reduction in the axial loading as described above. A suggestion on how this could happen is that the increase of the coefficient of friction, f, continued for a period of time after the friction force, Q, had stabilized.

It should be emphasized that the following analysis is only applicable to the push–pull loading of the specimen in Fig. 1, since bending deformation of the specimen introduces intolerable changes to the contact geometry.

3. COMPLETE FRETTING CONTACT OF WORN SURFACES

The minimum wear scar needed to obtain a uniform distribution in a fretting contact must be at least as deep as the difference between minimum and maximum depth according to eqn (3). Experiments carried out by Fernando *et al.* (1994) are reported to have a fretting scar of at least 3 μm under a fretting pad which is 1.27 mm wide. If a typical contact pressure of $p_0 = 100$ MPa is used in these tests where steel pads are pressed against an aluminium alloy, a wear depth of $h_{\max}-h_{\min} \approx 1.0$ μm is needed to get a constant pressure. The fact that the change of geometry needed to level out the contact pressure is smaller than the amount of wear observed in the experiments makes the assumption of uniform pressure distribution plausible.

3.1. *Shear stress distribution*

If the fretting pad continues to oscillate in a macro slip regime (i.e. the entire contact slides) as before the worn surface is developed, one obtains

$$|q(x)| = fp_0 \tag{4}$$

under the pad, i.e. the contact shear stress is uniformly distributed as before.

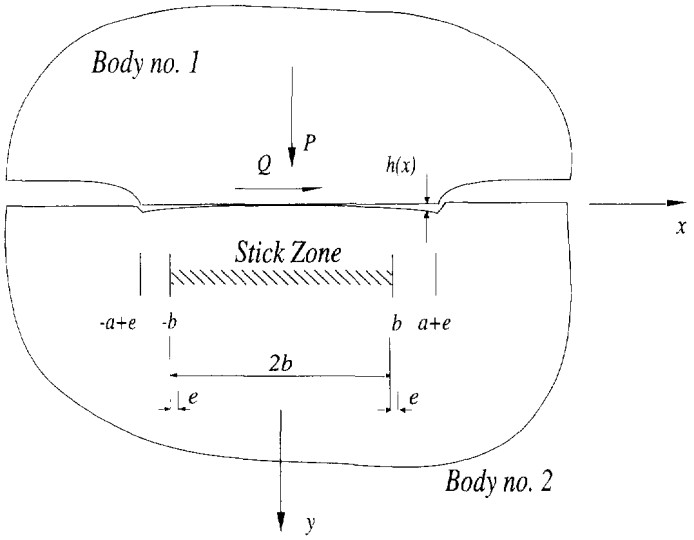

Fig. 2. Fretting geometry and measurement definitions.

For complete stick $g(x) = 0$ and hence $\partial g/\partial x = 0$ in the whole contact area. Equation (1b) and (A3) in the appendix then give the following solution to the shear stress distribution:

$$q(x) = \frac{C+\beta p_0(x-e)}{\sqrt{a^2-(x-e)^2}} \tag{5}$$

where e is the eccentricity of the stick zone such that the slip zone increases in size to $a-b+e$ on the right side of the stick zone and shrinks to $a-b-e$ on the left side as defined in Fig. 2. This solution gives infinite stresses at the edges of the contact patch which violates the friction law. Hence it must be assumed that when a friction force is applied, slip must take place at the edges.

For partial slip the contact patch is divided into a stick zone ($|x| \leqslant b$) and a slip zone ($-a+e \leqslant x \leqslant -b$ and $b \leqslant x \leqslant a+e$) as defined in Fig. 2 where eqn (4) is still valid in the slip area. In the stick area $g(x) = 0$. The distribution of contact shear stresses is now assumed to be

$$q(x) = fp_0 - q'(x) \tag{6}$$

where $q'(x)$ is the reduction of shear stress compared to the friction law, eqn (4), in the stick zone. Substitution of eqn (6) into eqn (1b) gives

$$\frac{1}{\pi}\int_{-b}^{b} \frac{q'(s)\,\mathrm{d}s}{s-x} = -\frac{fp_0}{\pi}\ln\frac{a-e+x}{a+e-x} - \beta p_0 \equiv k(x). \tag{7}$$

Equation (7) is classified as a Cauchy singular integral equation where the solution varies with boundary conditions for $q'(x)$. Here the function $q'(x)$ should be zero at $x = \pm b$ and from eqns (A2) and (A4) we get the following solution satisfying both eqn (7) and the boundary condition

$$q'(t) = \frac{fp_0}{\pi^2}\sqrt{1-t^2}\left[\int_{-1}^{1}\frac{\ln\dfrac{1-\varepsilon+\alpha s}{1+\varepsilon-\alpha s}}{\sqrt{1-s^2}(s-t)}\,\mathrm{d}s+\pi\frac{\beta}{f}\int_{-1}^{1}\frac{\mathrm{d}s}{\sqrt{1-s^2}(s-t)}\right] \tag{8}$$

where $t = x/b$, $\alpha = b/a$ and $\varepsilon = e/a$. The Cauchy Principal Value of the first integral of the right-hand side is determined by the calculus of residues and the result defined as $I(\alpha, \varepsilon, t)$ is quoted here

$$\begin{aligned} I(\alpha,\varepsilon,t) &= \Pr V\int_{-1}^{1}\frac{\ln(1-\varepsilon+\alpha s)-\ln(1+\varepsilon-\alpha s)}{\sqrt{1-s^2}(s-t)}\,\mathrm{d}s \\ &= \frac{2\pi}{\sqrt{1-t^2}}\left(\arctan\frac{\alpha\sqrt{1-t^2}}{x^- +\alpha t}+\arctan\frac{\alpha\sqrt{1-t^2}}{x^+ -\alpha t}\right) \quad |t|\leqslant 1, \quad |\varepsilon|\leqslant 1-\alpha \end{aligned}$$

where x^- and x^+ are defined as

$$\begin{aligned} x^- &= 1-\varepsilon+\sqrt{(1-\varepsilon)^2-\alpha^2} \\ x^+ &= 1+\varepsilon+\sqrt{(1+\varepsilon)^2-\alpha^2}. \end{aligned}$$

The second integral on the right-hand side of eqn (8) is identically zero, thus

$$q(t) = fp_0\left[1-\frac{2}{\pi}\left(\arctan\frac{\alpha\sqrt{1-t^2}}{x^- +\alpha t}+\arctan\frac{\alpha\sqrt{1-t^2}}{x^+ -\alpha t}\right)\right] \tag{9}$$

with the same limitations on ε as above. Equation (8) is a valid solution to eqn (7) only when an additional consistency requirement from eqn (A4c) expressed as

$$\int_{-b}^{b}\frac{k(s)}{\sqrt{b^2-s^2}}\,\mathrm{d}s = 0$$

is satisfied. This consistency equation gives a relation between the stick zone size and eccentricity and the degree of dissimilarity of the contacting bodies when $k(s)$ is replaced by the right-hand side of eqn (7). After integration we get

$$\ln\frac{x^+}{x^-} = \ln\frac{1+\varepsilon+\sqrt{(1+\varepsilon)^2-\alpha^2}}{1-\varepsilon+\sqrt{(1-\varepsilon)^2-\alpha^2}} = \pi\beta/f \tag{10a}$$

with the special case of $\alpha = 0$ explicitly solved

$$\varepsilon = \frac{\exp(\pi\beta/f)-1}{\exp(\pi\beta/f)+1}. \tag{10b}$$

The eccentricity ε is plotted as a function of normalized stick zone size α for different values

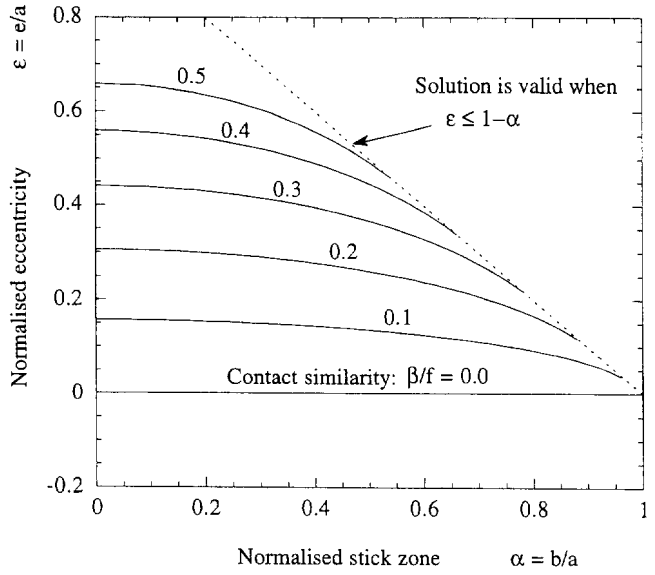

Fig. 3. Asymmetry of the stick zone for different material combinations (β/f).

of β/f in Fig. 3. It is seen that no eccentricity occurs when similar materials are in contact. It is also seen that for engineering materials where realistically $\beta/f \leqslant 0.3$, the eccentricity of the stick zone is 22% of the pad width at the limit of full sliding. If the material is exposed to an additional strain, ε_2, parallel to the contact surface, eqn (10a) will change to

$$\ln\frac{x^+}{x^-} = \frac{\pi}{f}\left[\beta + \frac{\varepsilon_2}{p_0 A}\right]$$

which represents a shift of the stick zone eccentricity. Equilibrium of contact shear stresses requires

$$2aq_0 \equiv Q = \int_{-a+e}^{a+e} q(x)\,\mathrm{d}x = 2afp_0 - \int_{-b}^{b} q'(x)\,\mathrm{d}x. \tag{11}$$

When eqn (8) is substituted into this equation the "tangential force coefficient" defined by Nishioka and Hirakawa (1969) appears as

$$\frac{q_0}{fp_0} = 1 - \frac{\alpha}{2\pi^2}\int_{-1}^{1} \sqrt{1-t^2}\, I(\alpha, \varepsilon, t)\,\mathrm{d}t \tag{12}$$

Since eqn (10a) gives a relation between α and ε for different material combinations represented by (β/f) the tangential force coefficient (q_0/fp_0) can be determined as a function of the normalized stick zone size α. Figure 4 shows this relation for different material combinations.

The distribution of shear stresses is available from eqn (9), but for an arbitrary combination of load level, Q and P, and material properties, β, the stick zone size and eccentricity must be determined first by combining eqns (10a) and (12).

For contact of similar materials eqns (9) and (12) reduce to

$$q(x) = fp_0\left(1 - \frac{2}{\pi}\arctan\sqrt{\frac{b^2-x^2}{a^2-b^2}}\right) \tag{13}$$

and

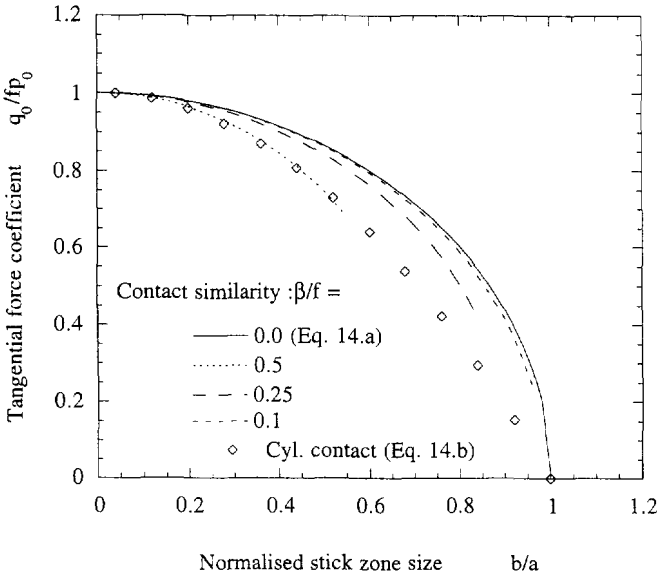

Fig. 4. Average shear stress normalized with respect to maximum shear stress for different stick zone sizes and material combinations (β/f).

$$\frac{q_0}{fp_0} = 1 - \frac{\alpha}{\pi}\int_{-1}^{1} \arctan\alpha\sqrt{\frac{1-s^2}{1-\alpha^2}}\,\mathrm{d}s = \sqrt{1-(b/a)^2} \tag{14a}$$

respectively. It is seen later that eqn (14) represents a good approximation of eqn (12) for realistic values of β. This simplifies the search for the stick zone size and eccentricity considerably. Nishioka and Hirakawa (1969) found the relation

$$q_0/fp_0 = 1-(b/a)^2 \tag{14b}$$

to be valid between the adhesive region and the tangential force coefficient, and is compared with eqn (14a) in Fig. 4. The authors confirmed this model with experimental observations for this contact geometry, and similar experiments are recommended for the case of the complete contact [eqn (14a)].

3.2. *Slip amplitudes*

Since the distribution of shear stresses is in principle known in the entire contact zone, eqn (1b) can be used to evaluate the relative displacement between the contacting bodies. We get

$$\frac{1}{Afp_0}\frac{\mathrm{d}g}{\mathrm{d}x} = \frac{\beta}{f} + \frac{1}{\pi}\ln\frac{a-e+x}{a+e-x} - \frac{1}{\pi^3}\int_{-1}^{1}\frac{\sqrt{1-s^2}I(\alpha,\varepsilon,s)}{x/b-s}\,\mathrm{d}s. \tag{15}$$

When eqn (10) and $I(\alpha, \varepsilon, t)$ is substituted into eqn (15), the maximum relative displacement is obtained by setting $\alpha = 0$, and g is denoted g_0 in this case:

$$\frac{\pi}{fp_0A}\frac{\mathrm{d}g_0}{\mathrm{d}x} = \ln\frac{a+e}{a-e} + \ln\frac{a-e+x}{a+e-x}. \tag{16}$$

The final point of stick is at $x = 0$ immediately before full sliding occurs. This gives $g_0(0) = 0$ as a boundary condition in the integration of eqn (16). The relative displacement between the two bodies is then given as

$$\frac{\pi}{fp_0A}g_0(x) = (a-e+x)\ln\left(1+\frac{x}{a-e}\right)+(a+e-x)\ln\left(1-\frac{x}{a+e}\right) \tag{17}$$

which gives a leading edge slip of

$$g_0(-a+e) = \frac{fp_0A}{\pi}2a\ln\frac{2}{1+\varepsilon} \tag{18a}$$

and a trailing edge slip of

$$g_0(a+e) = \frac{fp_0A}{\pi}2a\ln\frac{2}{1-\varepsilon}. \tag{18b}$$

It is seen that the leading edge and the trailing edge slip amplitudes are equal for contact of similar materials. In most fretting fatigue situations, the friction force oscillates with zero mean value. Therefore, the slip amplitude at the limit between full and partial slip can be estimated from eqns (18) as

$$\delta \equiv g_0(-a+e)+g_0(a+e) = \frac{2}{\pi}fp_0aA\ln\frac{4}{1-\varepsilon^2} \tag{19}$$

when δ is defined "from tip to tip" in the cyclic variation of the friction force. When $\alpha < 1$, partial slip occurs and $g(x)$ must be determined numerically from eqn (15). The slip amplitude can be normalized with respect to the slip amplitude at the edge of the contact at full slip:

$$\Delta = [g(-a+e)+g(a+e)]/\delta \tag{20}$$

which, of course, is unity on the verge of full slip. The relation between the tangential force coefficient, q_0/fp_0, and the normalized slip amplitude is illustrated for different degrees of dissimilarity in Fig. 5. These relations correspond to $\Delta \propto \ln(1-q_0/fp_0)$ suggested by Nishioka and Hirakawa (1969) which successfully described results from experiments using cylindrical contacts. As discussed in subsection 3.1, experiments could assess the relation

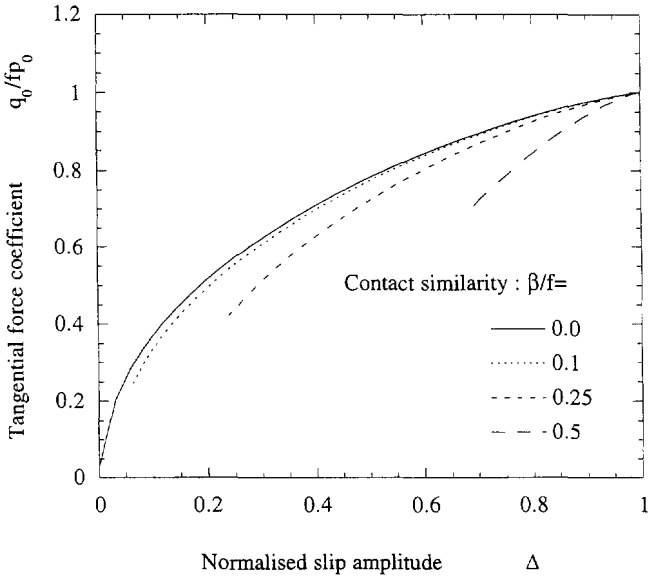

Fig. 5. The relation between the normalized slip amplitude and the tangential force coefficient for different material combinations (β/f).

Table 1. Stick zone size and eccentricity for contact between steel and aluminium for different friction coefficients, $Q = P/2$

f	q_0/fp_0	β/f	α	ε	$2f\Delta$
0.500	1.00	−0.220	0.000	−0.334	1.000
0.555	0.90	−0.198	0.416	−0.273	0.801
0.625	0.80	−0.176	0.579	−0.217	0.673
0.714	0.70	−0.154	0.695	−0.167	0.567
0.833	0.60	−0.132	0.784	−0.123	0.474
1.000	0.50	−0.110	0.854	−0.086	0.387

between the slip amplitude and the tangential force coefficient for the complete contacts described here.

4. BEHAVIOUR OF FRETTING CRACKS IN DIFFERENT SLIP REGIMES

To demonstrate the effect of stick zone size on the shear stress distribution in the partial slip regime of fretting experiments, the contact normal force, P, is chosen to be twice the contact shear force, Q. The coefficient of friction, f, is varied from case to case producing different amounts of slip in the fretting contact. When $f = 0.5$ the entire pad slides against the surface. But when f increases, a stick zone develops where the shear stress distribution is governed by eqn (9). A typical value of $\beta = -0.11$ is chosen (contact between aluminium and steel) and the stick zone size and eccentricity can be found. Based on this information on the stick zone, the amount of slip at the edges can be found by integrating eqn (15). Table 1 summarizes the development of stick zone size and eccentricity as well as the normalized slip amplitude for different coefficients of friction.

The stick zone size, α, and the eccentricity, ε, is found by numerically solving eqns (10a) and (12). For engineering purposes eqn (12) could be replaced by eqn (14), which would simplify the effort of finding α and ε. For the choice of loading conditions and material combination used here, the stick zone size would at the most be overestimated by 4.8% at $q_0/fp_0 = 0.9$.

Table 1 shows that an increase in the coefficient of friction causes the stick zone to grow and the relative displacement between the bodies to drop. This quite expected increase in the stick zone size produces a higher concentration of the contact shear stress at the edges of the contact as illustrated in Fig. 6. The development of the relative tangential displacement along the contact surface is also seen in the figure.

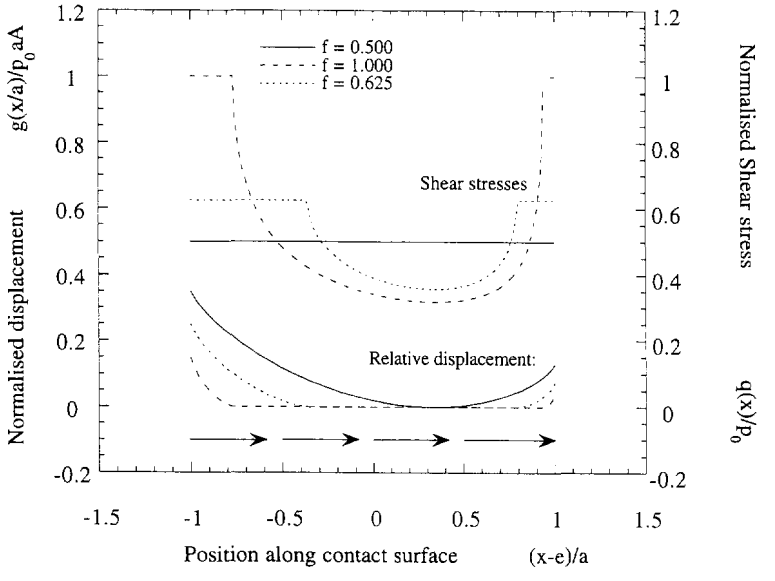

Fig. 6. Distribution of shear stresses and amount of slip in a fretting contact for different coefficients of friction when $Q = P/2$ and $\beta = -0.11$.

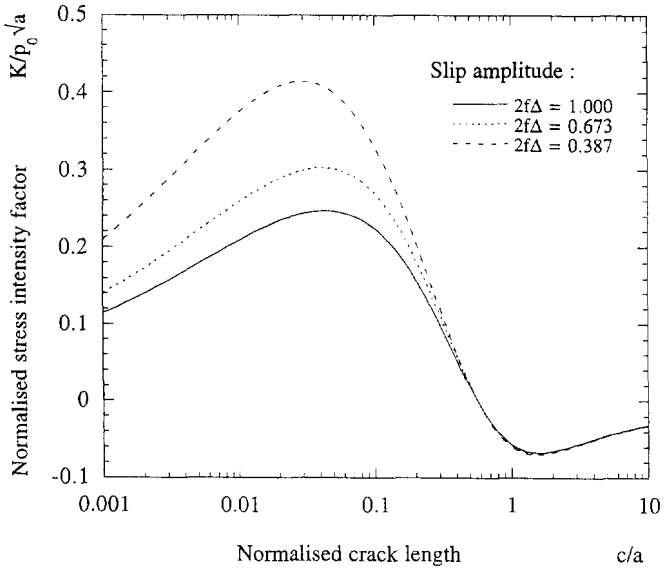

Fig. 7. Normalized stress intensity factors for $Q = P/2$ but different friction coefficients giving different sizes of the stick zone.

The mechanical loading of cracks in an overall linear material is conveniently represented by the stress intensity factor around the crack tip. Stress intensity factors for fretting cracks initiated at $x = -a+e$ may be calculated by using Green's weight functions

$$K_N^f = \frac{1}{\sqrt{2\pi c}} \int_{-a+e}^{a+e} \sigma_f(x) G_N^f(x, \theta)\, \mathrm{d}x \tag{21}$$

where $2c$ is the crack length, the index N = I, II for mode I and mode II stress intensity factors respectively, the index f = p, q for stress intensity factors caused by contact pressure and shear stress, respectively, θ is the angle defining the crack direction, σ_f is the distribution of contact pressure, $p(x)$, or shear stress, $q(x)$, and G_N^f is the Green's function for the appropriate contact load (f) and crack loading mode (N). Polynomial representations of the Green's function are found by Rooke and Jones (1979) for perpendicular cracks ($\theta = 0$) and by Rooke *et al.* (1992) for inclined cracks. Since a recent investigation (Faanes, 1995) shows that real crack paths can be accurately modelled by perpendicular cracks in most fretting situations, only perpendicular cracks are discussed here to simplify the analysis.

Mode I stress intensity factors of fretting cracks as a function of crack length are plotted in Fig. 7 for the loading examples shown in Fig. 6. It is seen that the highest stress intensity factors occur for low slip amplitudes for short cracks (< 50% of contact width). This implies that cracks should initiate earlier in contacts with the lower amount of partial slip and suggests that slip can have a beneficial effect compared to total stick! This was also discussed by O'Connor (1981) and is explained by the fact that a low slip amplitude corresponds to a high concentration of shear stresses at the edges of the contact.

The friction force measured at bridge pads increases until it reaches a "plateau" (Nix and Lindley, 1988) after a certain number of cycles in fretting experiments of the kind discussed here. If full slip continues to take place after this initial stage, the contact pressure and shear stress distribution is uniform according to the wear assumptions used here. In this case, no correlation can be seen between the amount of slip and the distribution of contact stresses, hence the mechanical loading of the fretting crack is unaffected by the slip amplitude. This agrees with the results obtained by Faanes and Fernando (1994a,b) where the fretting fatigue lives of the specimens were unaffected by the amplitudes of slip, and where good life predictions were obtained by assuming a uniform distribution of the contact stresses. Indeed, the investigators assumed that partial slip took place in some of the experiments, but this must be dismissed since the estimated slip amplitudes were much

higher than the theoretical limit of partial slip according to eqn (19). With a pad width of $2a = 1.27$ mm and a maximum shear stress of 125 MPa in the contact between steel and aluminium, eqn (19) gives a slip amplitude of approximately 2 μm while the amplitude always exceeded 6.7 μm in the experiments.

Table 1 demonstrates that for a certain global load in terms of P and Q, the size of the stick zone as well as the relative displacement between the bodies vary considerably with a change of coefficient of friction. This makes it difficult to determine the contact situation, since it may be hard to estimate the coefficient of friction in a fretting contact with sufficient accuracy. This problem is not present in the experiments with bridge type fretting pads reported here, since these tests are probably run under full slip conditions. Nevertheless it would be worthwhile to introduce partial slip in such experiments in the future. Hopefully, such experiments could clarify the relation between partial slip and fretting fatigue crack behaviour as indicated in this paper. It would also be interesting to compare partial slip experiments of this kind with those with incomplete contacts already described by, for instance, Hills and Nowell (1992). Partial slip is probably most easily achieved by reducing the frictional force after the initial stabilisation period as described above.

The stress distributions found in this paper as well as the Herz type pressures of incomplete contacts can now be compared with numerical techniques developed by Johansson (1994) where Archard's law of wear [e.g. Section 3.3.1., Sarkar (1980)] is implemented.

5. CONCLUSIONS

An elastic, closed form solution to the distribution of shear stresses in a contact with a uniform pressure distribution is developed. A uniform contact pressure may appear in fretting contacts where the contact geometry is modified by wear. The degree of partial slip can also be found in such fretting configurations.

The mechanical loading in terms of the stress intensity factor of a fretting crack varies with the degree of partial slip in the fretting contact. This is because the distribution of contact shear stress changes with different sizes and locations of the stick zone. The slip amplitude should therefore be seen as a secondary effect, and not as a direct cause to changes in the fretting fatigue crack behaviour. This conclusion remains to be confirmed by new experiments under partial slip conditions.

When fretting fatigue takes place under full slip conditions, the contact stress distributions are uniform, hence no correlation can be seen between the slip amplitude and the mechanical loading, and thus the crack growth behaviour, in this case.

Acknowledgements—The author wishes to thank F. Irgens for invaluable discussions during course of work. F. F. Knudsen's help with mathematical details is greatly appreciated.

REFERENCES

Dundurs, J. and Comninou, M. (1980). Shape of a worn slider. *Wear* **62,** 419–424.

Edwards, P. R. (1981). The application of fracture mechanics to predicting fretting fatigue. In *Fretting Fatigue* (Edited by R. B. Waterhouse). Applied Science Publishers.

Faanes, S. (1995). Inclined cracks in fretting fatigue. *Engng Fracture Mech.* **52,** 71–82.

Faanes, S. and Fernando, U.S. (1994a). Life predictions in fretting fatigue using fracture mechanics. In *Fretting Fatigue, ESIS* 18 (Edited by R. B. Waterhouse and T. C. Lindley), pp. 149–159. Mechanical Engineering Publications, London.

Faanes, S. and Fernando, U. S. (1994b). Influence of contact loading on fretting fatigue behaviour. *Fatigue Fracture Engng Mater. Structures* **17**(8), 939–948.

Fernando, U.S., Farrahi, G. H. and Brown, M. W. (1994). Fretting fatigue crack growth behaviour of BS L65 4% copper aluminium alloy under constant normal load. In *Fretting Fatigue, ESIS* 18 (Edited by R. B. Waterhouse and T. C. Lindley) Mechanical Engineering Publications, London (in press).

Hattori, T., Nakamura, M., Sakata, H. and Watanabe, T. (1988). Fretting fatigue analysis using fracture mechanics. *JSME Int. J.* Ser. 1, **31,** 100–107.

Hills, D. A. and Nowell, D. (1992). The development of a fretting fatigue experiment with well-defined characteristics. In *Standardization of Fretting Fatigue Test Methods and Equipment* (Edited by M. H. Attia and R. B. Waterhouse) ASTM STP 1159 pp. 69–84.

Hills, D. A. and Nowell, D. (1994). A critical analysis of fretting fatigue experiments. In *Fretting Fatigue, ESIS* 18 (Edited by R. B. Waterhouse and T. C. Lindley). Mechanical Engineering Publications, London (in press).

Hills, D. A., Nowell, D. and Sackfield, A. (1993). *Mechanics of Elastic Contacts*. Butterworth-Heinemann, Oxford.

Johansson, S. (1994). Numerical simulation of contact pressure evolution in fretting. *J. Tribol.* **116,** 247–254.
O'Connor, J. J. (1981). Elastic stress analysis of fretting fatigue failures. In *Fretting Fatigue* (Edited by R. B. Waterhouse). Applied Science.
Nishioka, K. and Hirakawa, K. (1969). Fundamental investigation of fretting fatigue—Part 5: The effect of relative slip amplitude. *Bull. JSME* **12**(52), 692–697.
Nix, K. J. and Lindley T. C. (1988). The influence of relative slip range and contact material on the fretting fatigue properties of 3.5NiCrMoV rotor steel. *Wear* **125,** 147–162.
Nowell, D. and Hills, D. A. (1987). Mechanics of fretting fatigue tests. *Int. J. Mech. Sci.* **29**(5), 355–365.
Rooke, D. P. and Jones, D. A. (1979). Stress intensity factors in fretting fatigue. *J. Strain Anal.* **14**(1), 1–6.
Rooke, D. P., Rayaprolu, D. B. and Aliabadi, M. H. (1992). Crack-line and Green's functions for stress intensity factors of inclined edge cracks. *Fatigue Fracture Engng Mater. Structures* **15**(5), 441–461.
Sarkar, A. D. (1980). *Friction and Wear*. Academic Press, London.
Switek, W. (1984). Early stage crack propagation in fretting fatigue. *Mech. Mater.* **3,** 257–267.
Tanaka, K., Mutoh, Y., Sakoda, S. and Leadbeater, G. (1985). Fretting fatigue in spring steel and carbon steel. *Fatigue Fracture Engng Mater. Structures* **8**(2), 129–142.

APPENDIX

Singular integral equations

To find $q(x)$ and $p(x)$ from eqns (1) the general formulation of the solution to a singular integral equation of the first kind can be used. The solutions are quoted from Table 5.2 in *Mechanics of Elastic Contacts* by Hills *et al.* (1993). The mathematical techniques lying behind these solutions can be found in the same reference.

If

$$\frac{1}{\pi}\int_{-a}^{a}\frac{f(s)}{s-x}\mathrm{d}s = k(x) \tag{A1}$$

then the unknown function $f(x)$ is given as

$$f(x) = -\frac{w(x)}{\pi}\int_{-a}^{a}\frac{k(s)\,\mathrm{d}s}{w(s)(s-x)} + Cw(x). \tag{A2}$$

The constant C and the function $w(x)$ are dependent on the characteristics of the solution in the end-points of the integration range.

If $f(x)$ is singular at both ends then

$$w(x) = \frac{1}{\sqrt{a^2-x^2}} \tag{A3a}$$

$$C \neq 0. \tag{A3b}$$

If $f(x)$ is nonsingular at both ends then

$$w(x) = \sqrt{a^2-x^2} \tag{A4a}$$

$$C = 0 \tag{A4b}$$

which is valid when the consistency requirement

$$\int_{-a}^{a}\frac{k(s)}{w(s)}\mathrm{d}s = 0 \tag{A4c}$$

is fulfilled.